ISSN 1840-4855
e-ISSN 2233-0046

Original scientific article
http://dx.doi.org/10.70102/afts.2025.1834.351

ENHANCED INDUSTRIAL VISION SYSTEM BASED TEXTURE CLASSIFICATION USING DCTP AND DPNN MODELS

N.P. Rajeswari[1*], Dr.M. Vijay[2]

[1]Assistant Professor, Department of Computer Science and Engineering, Velammal College of Engineering and Technology, Madurai, Tamil Nadu, India.*
e-mail: greatnpr@gmail.com, orcid: https://orcid.org/0009-0004-3890-6104
[2]Associate Professor, Department of Computer Science and Engineering, Kalasalingam Academy of Research and Education, Virudhunagar, Tamil Nadu, India.
e-mail: vijay.m@klu.ac.in, orcid: https://orcid.org/0000-0003-3337-815X

Received: August 30, 2025; Revised: October 13, 2025; Accepted: November 19, 2025; Published: December 30, 2025

SUMMARY

The paper will discuss the issues with industrial vision systems in detecting defects, especially in the manufacturing of tyres, where changes in exterior light and distortion will compromise the accuracy of defect detection. The suggested scheme combines Directional Convoluted Ternary Pattern (DCTP) in the extraction of texture features and Distributed Pattern-based Neural Network (DPNN) in the classification. The DCTP model aims to complement the border detection of tyre defects, resolving the problem of illumination and noise variations. The DPNN classifier with a distributed method of learning patterns of features has a significant effect on the model complexity; the prediction accuracy is increased by fewer training samples. The model was statistically verified using sensitivity (0.9862), specificity (0.9743), precision (0.9801), recall (0.9862), F1-score (0.982), accuracy (98.28), and Kappa coefficient (0.972). The mentioned metrics demonstrate a substantial improvement over the current models, such as YOLOv5, CNN, and SVM. The suggested DCTP-DPNN architecture is better than the conventional methods with the highest classification accuracy (up to 98 %) and the lowest error (2 %). These results demonstrate that the hybrid feature extraction method on the basis of texture and classification using neural networks is good for detecting tyre defects in industries in real-time.

Key words: *industrial vision system, defect identification, directional convoluted ternary pattern (DCTP), distributed pattern-based neural network (DPNN).*

INTRODUCTION

The fields of industrial automation, transportation systems, and product quality evaluation have seen significant changes in recent years due to the combination of computer vision and artificial intelligence. Industries are adopting sophisticated inspection and monitoring systems that can identify product faults and irregularities with little human involvement as a result of the growing need for safety, dependability, and operational efficiency. The prediction of abnormalities in the manufacturing products, such as the flaws in the surface of materials, holes, broken regions, etc., is more critical while manufacturing the product, considering the quality factor and maintaining the lifetime of the products, like tyres, and other

related products as referred in [1], when the external illumination changes while capturing the image of product or when the image was affected by the instrumentational noise, the detection accuracy will reduce because of the change in pixel intensity and intensity variation from the different projection of light. This makes the system misclassify the product, which reduces the accuracy of prediction, and crucial areas are missed due to the intense reflection from the surface of the object.

There are several advanced defect tracking systems that utilize the enhanced techniques of feature extraction, clustering, image segmentation, and classification with a deep learning model to analyze the defect parameters based on the enhanced statistical approach. In [2], the author defines the computer vision-based technologies, such as Convolutional Neural Network (CNN), Fast Region based CNN (FRNN), and You-Only-Look-Once (YOLO) model, which perform well based on the comparative analysis of the defect detection system. The industries, such as tyre manufacturing industries, textile industry, and other related hardware-based industries, verify the defect based on the surface variation since the defect detection in these types of industries varies in the texture pattern variations. Since improving the performance of prediction in the classification model requires a larger dataset to train, this results in an increase in time complexity and space complexity. As in the real-world dataset, the image might have affected by the environmental disturbances such as motion blur, light reflection, and illumination changes as referred from [3].

To overcome these problems, the proposed work integrates the texture-based object representation and classification, which is robust to external illumination changes. This proposed model enhanced the feature extraction process by verifying the pixel differences in terms of magnitude in various projections of angles. This texture-based feature extraction model refers to the light variation in various angles, which results in a normalized and enhanced boundary region of the object. The feature analyzed at various project angles refers to the fine intensity difference of object boundaries, which was robust in noise and background difference. This type of texture-based defect detection system in industrial applications enhances productivity and increases performance in quality analysis. The computer vision-based automatic monitoring system ensures safety compliance and a fast prediction model to reduce the time complexity in the manufacturing department.

The multi-directional-based texture pattern extraction model was implemented by using the Directional Convoluted Ternary Pattern (DCTP). As the name suggests, the algorithm can analyze the pixel difference in the image at different angles of projection. Also, the convoluted image pattern enhanced the object depth, which enhances the pixel borders. The defects, such as slight cuts, bubbles, broken regions, and other related flaws, can be highlighted by the DCTP model. This also enhanced the rotation invariant feature extraction technique to increase the prediction performance. This was enhanced from the Local Ternary Pattern extraction technique as referred from [4].

Similarly, the classification in this proposed work plays an important role in predicting the defects in an object. In [5], the deep learning model to predict the abnormalities required a large number of data samples to train the model, which leads to an increase in space and time complexity. In the proposed work, the neural network was enhanced based on the distribution model of the texture pattern, which improves the learning process. This was named as Distributed Pattern-based Neural Network (DPNN) to classify and detect the defective region of an object in the given testing image. This was effective in learning the training features with a minimum number of labelled data samples and their features. This optimizes the weights of neurons that form the hierarchical structure of the network formation with minimum error. From this, DPNN has the advantage of improved detection precision over the other existing models.

The comparative study of the proposed work shows the performance of classification by the evaluation of statistical parameters such as sensitivity, specificity, precision, recall, F1-score, MCC coefficient, accuracy, error rate, and kappa coefficient, which defines the number of correctly classified defects and the number of misclassifications recorded while in the testing phase. These parameters refer to the system's accuracy in prediction and scalability for industrial applications. The overall comparison analysis highlights the performance rate of the proposed work with the existing model.

This type of computer vision-based automation system focuses on the important issues in industrial applications. The improvement in production quality depended on the amount of training provided to the classification model. The main important goal of the combination of DCTP and DPNN was to reduce the training samples while increasing classification accuracy. This will also reduce the memory space of the training model and increase the speed of performance. The visual inspection technology reaches effective results in automatic quality analysis in terms of both methodology testing and performance of the overall system.

The objectives of the proposed work are listed as follows:

- To create a robust and accurate computer vision solution that can identify and track objects in dynamic environments.
- To analyze the quality of products in industrial applications based on imagery sensor data.
- To implement a novel texture pattern extraction method to represent the image texture feature using Directional Convoluted Ternary Pattern (DCTP).
- To train a novel classification model for improving the detection accuracy with fewer training samples using the Distributed Pattern-based Neural Network (DPNN).
- To validate the performance of the proposed methodologies based on statistical parameters and compare with existing algorithms.

Further, the work was organized in the structure as follows: The overview of the literature survey on the topics of texture feature extraction techniques and the neural network-based classification was described briefly in section II, with merits and demerits. The detailed explanation of the proposed model of DTP and DPNN, with algorithm steps and its mathematical representation, is explained in Section III. The overall performance of the proposed work was validated, and the prediction result was compared with existing methods in Section IV. In the result analysis section, the statistical parameters are evaluated and represented as tabular results and a graphical structure. Section V concludes the overall research work based on the implementation steps and the comparison report. In this section, the achievements of the proposed work are highlighted with the results and proofs that are evaluated. The future work of the proposed work is explained along with the conclusion part to describe the further enhancement process of the proposed work.

RELATED WORKS

This section presents the literature survey of existing techniques that are used in the industrial automation system of tyre fault identification based on computer vision with deep learning techniques. Based on this, Kazmi et al. [1] proposed an industrial automation system to detect the car tyre and recognize the text printed on the tire using convolutional neural networks (CNNs). This was to detect the text in the tyres in any case of light intensity changes with a pre-trained model of image variation due to environmental changes. Since the CNN-based model was to identify the text and locate it, which was considered a binary classification function, to improve it for multi-class tyre defect detection, Mohan et al. [2] proposed a multi-contrast convolutional neural network (MC-CNN) with quick feature integration with labelled attributes. Massaro et al. [3] presented a survey of different classification techniques that compare the performance range of Artificial Neural Networks (ANNs), K-means clustering, and Discrete Fourier Transform (DFT), which are involved in the prediction of tyre defects. From the overall comparison results, it was proven that the texture feature learning-based ANN classifier achieved better results than the other state-of-the-art methods.

Harshitha and Samala [4] proposed an enhanced CNN classification model by including edge identification with enhanced data pre-processing methods for detecting the tyre defects using the OpenCV development tool. Zhu et al. [5] proposed a machine learning based forecasting of the car tyre life span based on the visual effect of the tyre. Similarly, the Support Vector Machines (SVM) were used

to predict the life-span projection of the tyres and analyze the material parameters of the tyre manufacturing presented by Raj et al. [6]. This system identifies the flaws in the tyre based on the parameters such as the crack depth, width, intensity, and the volume of bulges present in the tyre. In addition to this, Pahinkar et al. [7] proposed Faster R-CNN trained by the training model of VGG16 for the multi-class defect detection in the tyre manufacturing industries.

In [8], Sharan et al. proposed the Multi-contrast CNN and Single Shot Detector (SSD) for implementing a vision task to monitor the multi-level sleepiness detection, which was integrated by the advanced vision concept of CNN. This study was useful for the investigation of computer vision technology by CNN to implement the tyre defect detection process. To increase the detection accuracy of the CNN technique, Rajeswari et al. [9] proposed the Weighted Quality-Based CNN (WQ-CNN) to reduce the computational complexity by means of optimizing the weight component of neurons in CNN. The signal analysis by Zhang et al. [10] demonstrates the advantage of a wave feature extraction model that predicts the structural defects from the product.

From the texture-based feature analysis, Ding et al. [11] were inspired by the textile defect monitoring system using the classification model of YOLOv5. From that, a dual-model prediction technique was implemented. Here, the lightweight object detection system was implemented to identify the defect in the tyre. A Feature Pyramid Network (FPN) was implemented by Yang et al. [12] to identify tyre speckles to spot the bubbles. This makes the enhancement of Faster R-CNN to achieve a high rate of recall and precision of prediction and classification accuracy. In [13], Wang and Wang enhanced the CNN model for detecting the tyre surface defect by integrating the Generative Adversarial Network (GAN). The TD-YOLOA was proposed by Peng et al. [14], which was an improved version of the YOLO network structure that integrates the high attention functionality for tyre defect detection. This was validated by comparing the result with the YOLOv5 model, which achieves an mAP parameter increased by 5%.

Taspinar [15] surveyed different pre-trained CNN architectures, such as VGG19 and ResNet50, to validate the tyres that are non-defective or the defective object that represents the advantages of the transfer learning function integrated with the sparse dataset. The machine learning model-based classifier was integrated with the feature extraction model by Histogram of Oriented Gradients (HOG) and Local Binary Pattern (LBP) presented by Liu et al. [16] to detect the tyre appearance fault. This type of texture-based hybrid feature extraction technique was interpretable and reduced the computational complexity. The InceptionV3 introduced by Kaushik et al. [17] approaches the smart tyre monitoring system, which integrates the high-level feature enhancement over conventional CNN-based techniques. The ResNet50 model was used in Kaushik et al. [18] to enhance the deep learning model for tyre quality classification. The result of the classifiers was compared with the other state-of-the-art methods, which show excellent resilience even at the uneven surface and dynamic change of illumination in an industrial environment.

Orowho and Vincent [19] proposed a hybrid combination of classifiers to predict the fault in the tyre. In this, the CNN features were combined with the Random Forest classifiers to maintain the parameters such as precision and recall in a balanced condition. This enhances the accuracy of CNN compared with the traditional combination of other classifiers. The classification technique of XGBoost and ensemble deep learning models was based on the combination of different existing state-of-the-art classifiers, which were integrated for multi-class prediction, and tyre quality analysis was proposed by Singh et al. [20]. Saleh and Ertunç [21, 23] introduced an attention-based deep learning algorithm for industrial tyre defect identification. This was implemented by the combination of local and global features of the image. This method of prediction system enhances the performance level of traditional CNNs by extracting the contextual features of the entire surface of the tyre. A lightweight and effective model for real-time defect identification in natural daylight, Tyre-YOLOv11n, was presented by Yuan et al. [22]. The parameters, such as scalability and other statistical values of the model, indicate that this model was suitable for embedded industrial systems. Similarly, an enhanced feature extraction technique for segmentation and classification of defective regions of the tyre was implemented by Li et al. [24]. This study focused on the fault identification for the input of radial tyre X-ray images utilizing impurity and cord defect analysis.

The summary from the literature can be described as the technologies that are enhanced from the traditional methods of defect identification by the use of deep learning architectures, such as ResNet, Faster R-CNN, and YOLO, which improved the feature extraction and prediction model. Some of the references are focused on the improvements in the algorithm, and some are on the methods for enhancing the prediction model in computer vision technologies. By considering the overall key points in this survey, texture-based image feature representation in the neural network classification model enhances the precision of the defect detection system and quality analysis in the tyre quality predictive maintenance system.

PROPOSED METHODOLOGY

In this proposed work, the tyre defect detection was enhanced by the combination of texture-based image feature representation and the neural network technology to classify and predict the defective region, which improves the sensitivity and the accuracy of prediction. Since the rotational invariant feature classification model predicts the defect at different intensity levels, it also includes other noises that are included in the captured image. Here, the Directional Convoluted Ternary Pattern (DCTP) was implemented to extract the texture pattern of the image and define the feature vector by representing the histogram of the extracted texture pattern. In the classification part, an enhanced neural network technology was introduced as a Distributed Pattern-based Neural Network (DPNN) that classifies the works based on the distributive analysis of extracted texture features of the image. Figure 1 shows the architecture diagram of the overall system module of the proposed work. This illustrates the flow of the proposed work, and the integrated blocks represent the steps that predict the defect in the tyre.

The main modules of this proposed work were the integration of DCTP and DPNN. The learning of the DPNN classifier considers the encoded features of the texture pattern that selects the combinations of similarity between the features to form the network structure between the best selected neurons. To make the right combinations of features for the class labels mapping, the feature attributes from the DCTP texture pattern were organized and normalized at the input layer of the DPNN classifier. The proposed method of DCTP-DPNN-based tyre recognition techniques optimizes the training parameters based on the distribution of the gradient features and their back propagation, which improves the prediction accuracy.

In this work, the modules of the proposed work are subdivided as follows.

- Pre-processing
- Pattern extraction (DCTP)
- Classification (DPNN)

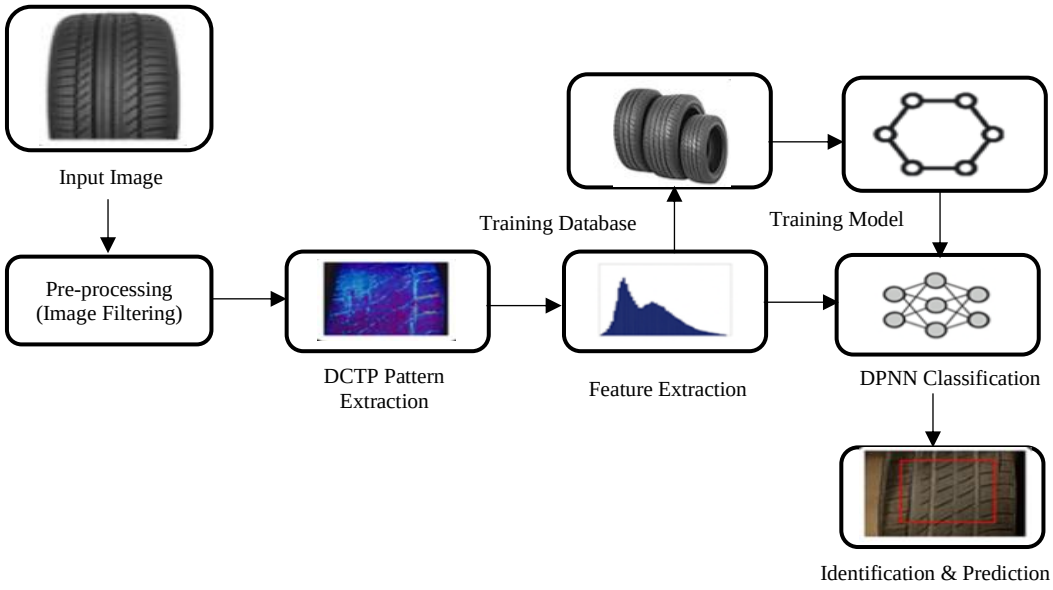

Figure 1. Architecture diagram of the proposed system

A. Image Pre-processing

The image pre-processing is recommended to improve the pixel quality of the image by filtering the noisy pixels that are present in the image matrix and enhancing the intensity of pixels based on the normalization factor. This type of pre-processing helps the system to detect the clear region of the boundary for an object, which improves the texture extraction. This filtering method improves the performance of classification and increases the prediction accuracy. This proposed work implements the image filtering to enhance the boundary region of the object and smooth the image using the Gaussian Normalized Denoising (GND) method. This filtering method refers to the neighboring pixels of the image matrix by considering the mask size that is projected to the image matrix. To apply the filter, this mask matrix was considered to estimate the difference among the boundaries of the image, normalize the mask, and replace the corrected pixel in the mask matrix. In the proposed model, the pixels that are affected by the noise can be represented as 'E_{xy}', which was defined by equation (1).

$$E_{xy} = \begin{cases} C_{ij}, & if\left(mean\left(T_{ij}\right) > I_{xy}\right) \\ 0, & Otherwise \end{cases} \quad (1)$$

Where 'I_{xy}' represents the image pixel matrix for the size index of x and y. From this, the 'X' and 'Y' ranges are referred to as

$$x = \{1,2,\dots M\};\ y = \{1,2,\dots N\} \quad (2)$$

In the size representation of 'x' and 'y', the parameter 'M' represents the row size and 'N' represents the column size of the image matrix. In the noisy pixel estimation referred from equation (2), the filter mask matrix 'T_{ij}' can be evaluated as in equation (3)

$$T_{ij} = E(x-1{:}\,x+1, y-1{:}\,y+1) \quad (3)$$

From the reference of filter mask matrix, the center pixel of the matrix 'I_c' represents the average difference value in T_{ij}, which normalizes the pixels in the mask and replaces them in the filter image mask based on the 'x' and 'y' coordinate position. Figure 2 shows the different sizes of filter masks that are considered in the filtering method. The size of the mask is differentiated as 5×5 and 3×3 matrix configurations to apply the filter. Among the different matrix sizes, the smaller the size of the mask matrix, the better the filtering effect on the image compared to the larger the size of the matrix.

i-2, j-2	i-1, j-2	i, j-2	i+1, j-2	i+2, j-2
i-2, j-1	i-1, j-1	i, j-1	i+1, j-1	i+2, j-1
i-2, j	i-1, j	i, j	i+1, j	i+2, j
i-2, j+1	i-1, j+1	i, j+1	i+1, j+1	i+2, j+1
i-2, j+2	i-1, j+2	i, j+2	i+1, j+2	i+2, j+2

(a) 5 × 5 matrices

i-1, j-1	i, j-1	i+1, j-1
i-1, j	i, j	i+1, j
i-1, j+1	i, j+1	i+1, j+1

(b) 3 × 4 matrix

Figure 2. Mask matrix for the filtering algorithm (GND)

The resultant filtered matrix '$I_f(x, y)$ ' can be represented as the collection of corrected or filtered pixels from the mask matrix. From this filtered image matrix, the image was passed to the texture feature extraction module as a grey-level converted image. From the analytical result of the filtering method tested with different noise levels, the proposed filtering method gains a better Peak Signal-to-Noise Ratio (PSNR) compared to the traditional filtering method. Figure 3 shows the sample result of the filtered image for the given test input. In that, row (a) represents the test images added with 10% of noise level, and row (b) shows the filtered result of the given images with the estimated PSNR in dB.

(a) Test Input

PSNR = 65.8 dB PSNR = 72.4 dB

(b) Filtered Image

Figure 3. Samples of filtered image

B. Pattern Extraction

The image, followed by the filtering module, was passed to the texture pattern extraction module, which was integrated by the Directional Convoluted Ternary Pattern (DCTP) method. To classify the defect classes and their types of defects, the DCTP algorithm proposed a novel texture pattern extraction technique based on a multi-directional boundary analysis method.

The filtered image, "I_f," is then passed to the texture pattern extraction function at different angles of projection. Initially, the texture pattern extraction method splits the image into multiple cell matrices to represent the center of the pixel and boundaries that move around the full image matrix. This cell matrix was in the size of 3x3. Before running the extraction of the texture pattern, the zero-padding was initialized over the image to prevent the loss of outer boundary pixels of the image. A mask window matrix with size 5x5 was initialized, which was represented as "I_W". This will estimate the difference in the neighborhood pixels of each boundary pixel of the cell matrix. This helps to find the difference in multiple directions, as shown in Figure 4.

The DCTP algorithm estimates the pixel difference in five different angles of projection as {+90∘, +45∘, 0∘, −45∘, −90∘}. This was estimated at each window matrix projected over the cell boundary pixels. Since the image was convoluted before the analysis of pixel difference, the pattern will enhance the object texture. This type of texture feature extraction method estimates the fine difference between each pixel and its boundaries to represent the clear texture of an object. The result of DCTP was the encoded format of the difference in pixels and rearranged into a matrix, similar to an image. This matrix will represent the texture pattern of the testing image. Then the histogram of that texture was evaluated to form the feature vector of the testing image.

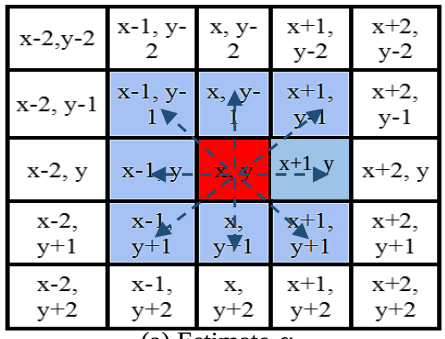

(a) Estimate α_c

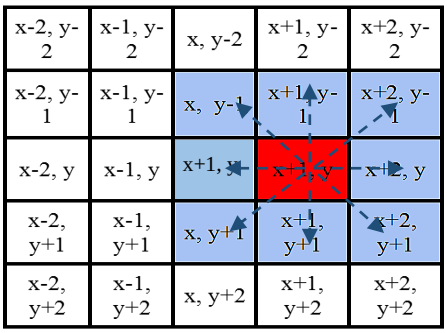

(b) Estimate α_k

Figure 4. Phasor diagram of DCTP

Figure 4 shows the phasor diagram of the DCTP texture pattern extraction model. In that, the 'x' and 'y ' represent the row and column of each cell matrix. In this cell matrix, the coordinate position was highlighted in red, representing the center pixel of the cell, and the other blue colored coordinate positions represent the boundary pixels of the cell. The arrow mark shows the direction of difference identification between the center pixel and the boundaries. Algorithm 1 describes the step-by-step procedure of the proposed DCTP texture pattern algorithm.

Algorithm - 1: Directional Convoluted Ternary Pattern (DCTP)

Input: Filtered image 'I_f'.

Output: Texture pattern 'T_{DCTP}' and feature vector 'F_v'.

Step 1: Read the grayscale image of the filtered image $_{,if}\ (x, y)$ with zero-padding.

Step 2: Initialize the radius of neighbourhood pixels $R = 3$.

Step 3: Compute ternary comparison between each neighbour and centre related to the threshold 'Th'.

For ii = 2 to (m-1)

For jj = 2 to (n-1)

// Loop runs for '(m-1)' row and '(n-1)' column size of image to define each pixel in the image as the centre of the sub-mask matrix 3×3.

Step 4: Estimate the centre pixel 'g_c' of the sub-mask and neighbouring 'g_k' of the mask matrix from (4) and (5) respectively.

Step 5: Generate the ternary pattern 'TP' from the magnitude difference 'M' from equations (6) and (7), respectively.

Step 6: Split the Ternary pattern into $TP^+$and TP^- (9) and (10). For each direction 'd', convolve TP^+ and TP with the directional vector V_d.

Let the direction for extracting the pattern 'd' can be defined as in equation (11).

Step 7: Convolve the ternary patterns 'C_d' (12) and (13) with the directional kernels at each direction 'd'.

Step 8: Identify dominant direction for positive 'd^+' and negative patterns 'd^-' from (14) and (15).

Step 9: Encode directional responses to form DCTP code '$T_{DCTP}(ii, jj)$' from equation (16).

Step 10: Accumulate a histogram of DCTP codes over the texture pattern to represent the feature vector 'F_v' of the given testing image from equation (19).

Step 11: Use the histogram as a texture feature vector and end the loop.

End 'jj' loop

End 'ii' loop

Let the filtered image 'I_f' be considered as the input image for the algorithm, and ' m 'and 'n' are the row and column sizes of the image matrix. This was normalized by converting the RGB image to a greyscale for a single sample of the image to extract the texture pattern. In this, the cell size was considered as 3x3, the radius of the boundary 'R' was specified as 3. Since the cell size was considered as 3, the zero-padding for the image matrix was applied to 1 layer outside the matrix.

The loop for cell validation will run from 2 to the size of '(m-1)' and '(n-1)'. This considers only the centre pixel of the cell matrix, separated from the whole image matrix. Based on the index of 'ii' and 'jj', the g_c and g_k can be calculated as in equations (4) and (5), respectively.

$$g_c = I_f(ii, jj) \quad (4)$$

$$g_k = I_f\left(ii + Rcos\left(\frac{2\pi k}{K}\right), jj + Rsin\left(\frac{2\pi k}{K}\right)\right) \quad (5)$$

Where:

$k = 1,2, \dots, K$

K – Length of the boundary pixels of the mask matrix.

As the mask matrix size was 3×3, the size of the boundary pixel 'K' can be defined as 8. From the mask matrix, the ternary pattern TP was calculated from the Magnitude difference of the center pixel and the boundaries. The '*TP*' and '*M*' are represented as in equations (6) and (7), respectively.

$$TP = \{M(g_0 \sim g_c), M(g_1 \sim g_c), \dots M(g_{K-1} \sim g_c)\} \quad (6)$$

$$M(g_k \sim g_c) = \begin{cases} +1, & g_k \geq g_c + Th \\ 0, & |g_k - g_c| < Th \\ -1, & g_k \leq g_c - Th \end{cases} \quad (7)$$

Where:

The threshold 'Th' can be calculated as the average of the boundary pixels of the mask matrix (Equation 8).

$$Th = \frac{\sum g_k}{K} \quad (8)$$

The TP contains the set of matrices with both positive and negative differences of the Ternary pattern. To encode the texture pattern, this needs to be split into TP^+ and TP^- to represent the texture in two directions. This can be represented in equations (9) and (10) respectively.

$$TP^+(k) = \begin{cases} 1, & M(g_k \sim g_c) = +1 \\ 0, & Otherwise \end{cases} \quad (9)$$

$$TP^-(k) = \begin{cases} 1, & M(g_k \sim g_c) = -1 \\ 0, & Otherwise \end{cases} \quad (10)$$

Since the Ternary pattern has the magnitude of difference in pixels, the pattern can be improved by convoluting the mask matrix with the directional vector 'V_d'. In this, the 'd' represents the direction of pattern in different angles to extract the ternary difference in neighbouring pixels. The convoluted matrix of mask with direction vector at positive ternary and the negative ternary difference are represented in equations (12) and (13).

$$d = \{0°, 45°, 90°, 135°, 180°\} \quad (11)$$

$$C_d^+(ii, jj) = (TP^+ * V_d)(ii, jj) \quad (12)$$

$$C_d^-(ii, jj) = (TP^- * V_d)(ii, jj) \quad (13)$$

Where 'V_d' was defined from the Kirsch mask.

Similarly, the dominant direction of the pattern can be updated at each iteration and can be denoted as 'd^+' and 'd^-'. This can be referred to by equations (14) and (15),

$$d^+(ii, jj) = arg\ max\left(C_d^+(ii, jj)\right) \quad (14)$$

$$d^{-}(ii,jj) = arg\ max\left(C_{\bar{d}}^{-}(ii,jj)\right) \quad (15)$$

From the dominant direction, the index of maximum value of the convoluted ternary pattern was identified and arranged in a vector for the encoding process. In parallel to that, the overall texture pattern 'T_{DCTP}' of the DCTP was identified by collecting both the positive and the negative ternary patterns and merging by encoding the boundary differences to get the texture pattern of the DTP algorithm. This was represented in the equation (16).

$$T_{DCTP}(ii,jj) = \sum_{d=0}^{D-1}[b_d^{+}(ii,jj) \times 2^d] + \sum_{d=0}^{D-1}[b_d^{-}(ii,jj) \times 2^d] \quad (16)$$

Where, b_d^{+} and b_d^{-} are can be defined as the binary representation of the direction vector comparing with dominant direction as in (17) and (18).

$$b_d^{+}(ii,jj) = \begin{cases} 1, & d = d^{+}(ii,jj) \\ 0, & otherwise \end{cases} \quad (17)$$

$$b_d^{-}(ii,jj) = \begin{cases} 1, & d = d^{-}(ii,jj) \\ 0, & otherwise \end{cases} \quad (18)$$

From the resultant matrix of '$T_{DCTP}(ii,jj)$', the texture pattern was extracted and visualized as an indexed image to represent the depth of intensity difference and the impression of the object in the image. For the further classification process, the texture pattern matrix needs to be represented as a feature vector. For this process, evaluate the histogram of the texture image as in equation (19)

$$F_v = \sum_{ii,jj} \delta(T_{DCTP}(ii,jj) = H) \quad (19)$$

Where 'δ' is the histogram function

$H = \{0, 2, 3, \ldots, 255\}$

This form of histogram feature vector is extracted for all the training image datasets and arranged in rows to form the training database. Figure 5 shows the texture pattern of the filtered image.

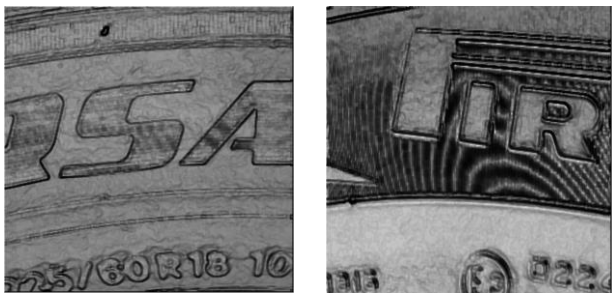

Figure 5. Texture pattern of filtered image

C. DPNN Classification

To classify an image, the classifier needs to select based on the requirements and the classification labels of an object. Since the classifier can be categorized as a binary classifier and a multi-class classifier based on the training labels that are provided to the model. If the object needs to be classified as only a fault or a non-fault object, then the binary classifier is sufficient to classify the testing object. Since this will not give more information to specify the fault type, such as crack, broken piece, flattened area, etc., and other related defects. Here, the multi-class classifier was selected and used to classify the multiple defect types present in the Region of Interest (ROI) of the object.

In the proposed work, the tyres are classified by the multi-class classifier to identify the detection types using a Distributed Pattern-based Neural Network (DPNN) classifier to predict the different labels of faults from the extracted ROI of image features. The proposed DPNN classifier was implemented and tested in the YOLOv5 tyre image dataset, at various external illumination changes and with additive noise to the image. Since the dataset contains images that are captured in different situations of defective tyres and non-defective tyres, it helps to analyze the algorithm in various situations. The network formation and the arrangement of neurons based on the kernel function of the classifier differ from traditional neural network classifiers. This enhances the prediction performance in terms of accuracy and sensitivity-related parameters.

The proposed DPNN classifier integrates the distribution function to evaluate the relevance of a feature in both the training and testing processes. This forms the hierarchical combination of neuron structure based on the texture feature attributes of the feature database. While in the training process, the neurons can learn the combination of features and the correlation between the attributes of a defective object and its characteristics. It learns about the difference in weight and how it is interlinked to the features to form the network combination. This form of learning the feature attributes will reduce the error rate. In parallel to that, the classifier can identify the matching relationship between the training model and the testing features. This combination of distribution function-based identification with the sophisticated texture feature extraction method improves the prediction performance compared to other state-of-the-art methods.

The estimation of probability training and testing probabilities based on the data points was implemented to classify the selective attributes of features from the database. The class label "L" can be shown as follows:

$$L = \arg\min(\rho(K, K_r)) \tag{20}$$

In Equation 20, where: $\rho(K, K_r)$ - Probability of feature vector.

$$U(ij) = U(\theta_i, \theta_j) \tag{21}$$

In Equation 21, where $U(ij)$ - Vector of Parzen kernel function and θ represent the angle between the vector points at 90̊

$$'i' and' j' \in \{1,2,..., N\}$$

$$F_s(Ui) = \sum_{j=1}^{R} U(ij) F_s(j) \tag{22}$$

$$F_s{}^r(Ui) = \sum_{j=1}^{R} U(ij) F_s{}^r(j) \tag{23}$$

In Equations (22 & 23), where: R - Feature size.

Equations (24) & (25), then, may be used to pick the sub-vector of feature update S and Sr $F_s(Ui)$ $F_s{}^r(Ui)$, respectively.

$$S = F_s(i) \ln\left(\frac{2 \times F_s(Ui)}{F_s(Ui) + F_s{}^r(Ui)}\right) \tag{24}$$

$$S^r = F_s{}^r(i) \ln\left(\frac{2 \times F_s{}^r(Ui)}{F_s(Ui) + F_s{}^r(Ui)}\right) \tag{25}$$

These feature vector learning procedures measure the separation between the neuronal weight values as

$$\rho(K, K_r) = \sum_{i=1}^{h} \left(S + S^r\right) - \ln(p_r) \quad (26)$$

In Equation 26, where: p_r - Probability of hypothesis vector.

The output layer of the classifier identifies the similarity between the trained features of the database and maps them to the categories of defect labels from the actual trained data. The similarity result represents the predicted label of the given testing image. Since the histogram features of the testing image are used to classify and detect the depth pattern at each pixel intensity, and identify the relevance of the defect region. The encoded structure of the connected neuron structure at the input layer and the hidden layer is based on the kernel function of the proposed neuron network architecture. This form of color map representation for the feature prediction process presents an intuitive comprehension of the DPNN algorithm to form the combination of network formation.

The overall classified results state that the combination of texture pattern with the distribution model of neural network technologies enhanced the classification accuracy in the type defect identification system. The proposed DTP-DPNN algorithm improves the model's decision-making function to classify and label defective objects in an image. The results and discussion presented in this section present the comparison of performance parameters and statistical analysis based on the validation of predicted and ground truth of the dataset.

RESULTS AND DISCUSSION

The proposed system was executed with the help of Python, TensorFlow, and Keras libraries to develop and train a model. Directional Convoluted Ternary Pattern (DCTP) image pre-processing and feature extraction were done through OpenCV and self-written scripts. Distributed Pattern-based Neural Network (DPNN) was trained with the help of the deep learning capabilities of TensorFlow and its ability to train models efficiently. Other existing classifiers, like CNN and SVM, were also tested using the PyTorch framework using the FYOLOv5 model. All the experiments were done through a machine with an NVIDIA GPU to process and evaluate the models at a faster rate.

In this section, the overall results of the proposed work of DCTP-DPNN were tested and analyzed for the YOLOv5 image dataset. The dataset contains collections of tyre images with various tyre fault types, such as cracks, bulges, cuts, and surface wear, which are labelled with the ground-truth. From the collections of image datasets, the proposed work was tested in different environments, such as outer illumination changes, additive instrumentation, and environmental noise to the image, different resolutions, and multiple defect features that are available in the image dataset. The YOLOv5 image dataset contains 828 good tyres and 1028 defective/faulty tyres. A total of 1856 images are collected in the dataset. From the overall dataset, 70% was considered for the training data, and the remaining 30% of each class was considered for testing the proposed method.

Table 1. Experimental Parameters for Tyre Defect Detection

Parameter	**Value**
Dataset Split	70% training, 30% testing
Feature Extraction	DCTP (5 angles)
Classifier	DPNN
Optimizer	Adam
Learning Rate	0.001

Table 1 shows the important parameters applied in the experiments to test the proposed DCTP-DPNN model to identify tyre defects. These parameters specify the dataset, feature extraction procedure, classification model, and training parameters used to facilitate consistency and transparency in the evaluation procedure.

The validation process was measured by the wide range of statistical parameters, such as Sensitivity (True Positive Rate), Specificity (True Negative Rate), Precision, Recall, Accuracy, F1-Score, Matthews Correlation Coefficient (MCC), and Cohen's Kappa Coefficient, that are to measure the performance rate of proposed work compare to the other existing methods that are analyzed with the same dataset.

Based on these experimental data, the proposed DCTP-DPNN algorithm performs better accuracy than the other methods, like YOLOv5 with a basic model of classifiers, Convolutional Neural Networks (CNN), and Support Vector Machines (SVM). The result proves that the proposed model performs well with a smaller number of image training. The texture pattern extraction of the DTP method enhances the unique features of the object that are present in the image. The sample results at each stage of the proposed work are shown in Figure 6. In this figure, the first row shows the testing of DCTP-DPNN for a good tyre, and the second row shows the testing of DCTP-DPNN for a faulty tyre. Each column represents the Input Image, Filtered Image, DCTP Texture Pattern, and Histogram Feature, respectively.

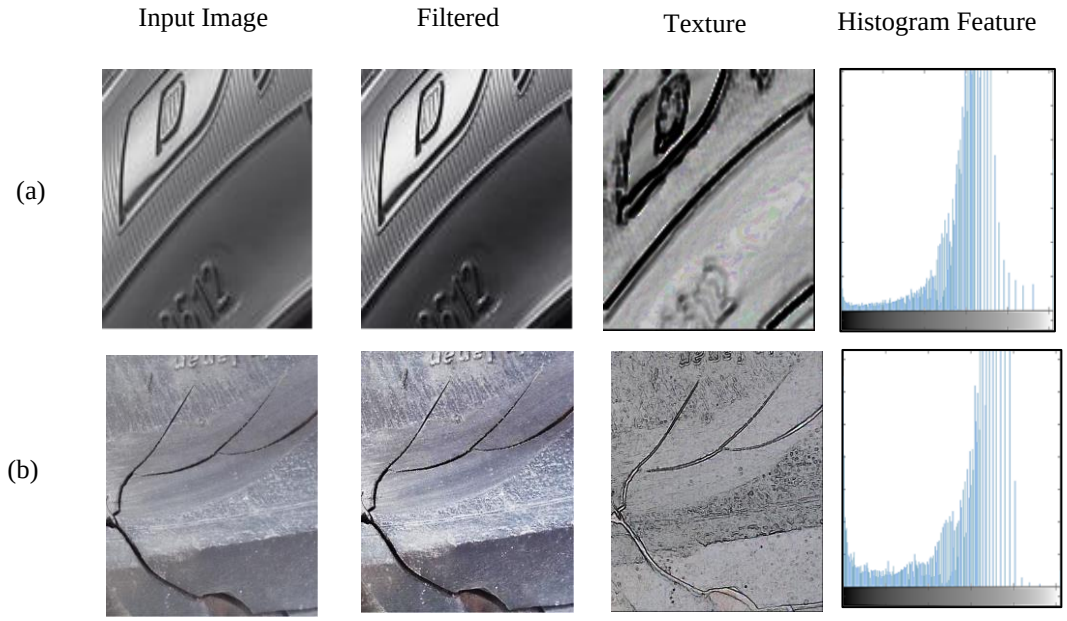

Figure 6. Sample test result of proposed work. (a) Good tyre, (b) Defective/Fault tyre

D. Performance Indicators

The performance measures are taken into account by evaluating the statistical parameters by comparing the predicted result with the ground-truth of the image dataset. The mathematical representation of all the statistical parameters is followed in the equations (27) through (37).

$$Sensitivity, TPR = \frac{True\ Positive\ (TP)}{TN+FN} \quad (27)$$

$$Specificity, TNR = \frac{True\ Negative\ (TN)}{TN+FN} \quad (28)$$

$$Jaccard, J = \frac{TP}{TP+FP+FN} \quad (29)$$

$$Dice\ Overlap, D = \frac{2J}{J+1} \quad (30)$$

$$Precision, P = (1 - FDR) = \frac{TP}{TP+FP} \quad (31)$$

$$Recall, R = (1 - FNR) \quad (32)$$

$$F1\ Score, F\_S = \frac{2TP}{2TP+FP+FN} \quad (33)$$

$$MCC = \frac{TP \times TN - FP \times FN}{\sqrt{(TP+FP)(TP+FN)(TN+FP)(TN+FN)}} \quad (34)$$

$$Accuracy, Acc = \frac{Total\ correct\ labels}{/Total\ No.of\ Samples} \quad (35)$$

$$Error\ (\%) = (100 - Accuracy\%) \quad (36)$$

$$Cohen's\ Kappa = 1 - \frac{(1-P_o)}{(1-P_e)} \quad (37)$$

Where: P_o – Probability of Relative observation,

P_e – Hypothetical probability,

TP – True Positive,

TN – True Negative,

FP – False Positive,

FN – False Negative.

The proposed DCTP–DPNN tyre fault detection model's overall performance evaluation is validated by the comparison of the existing model, which is referred from the papers [23]. The parameters are evaluated, and the comparisons are presented in the table result and graphical representation to visualize the performance results. Based on the evaluated value and the peak measurement of each parameter, the achievement of the proposed work is shown in the overall result table. To make a clear visualization of comparison, the parameters are plotted in a bar chart to represent the peak variation among methods. These table and Figure 7 shows the comparison result in terms of accuracy and false rate identification, where the methods are effective in the worst-case scenario. Increasing the value of accuracy will reduce the value of the error rate.

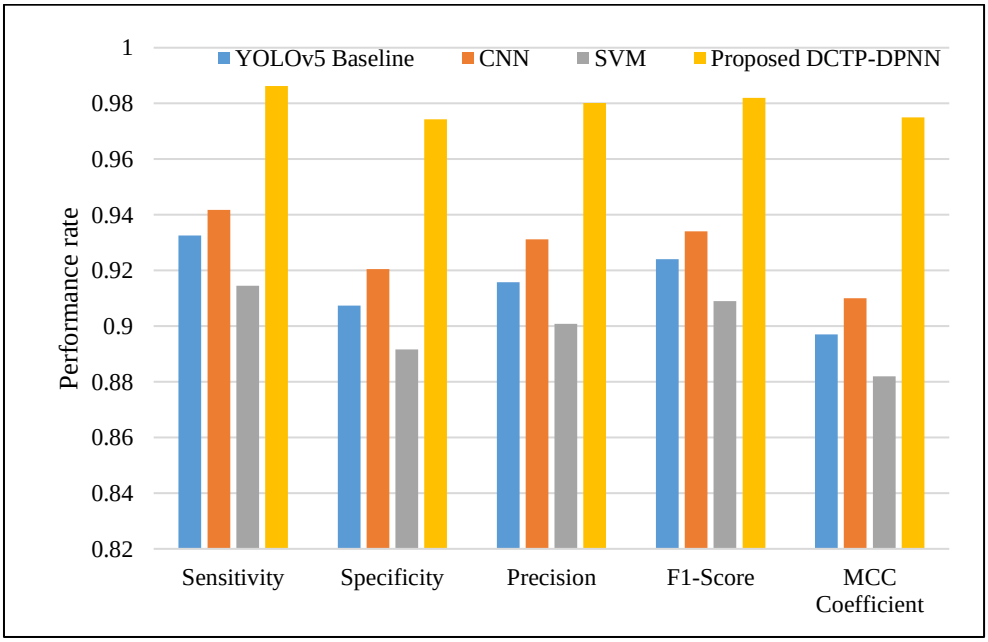

Figure 7. Performance measures

Table 2 presents the relevant numerical values of these parameters, as well as the total classification accuracy, in addition to the graphical findings. A greater quantitative grasp of the gains made possible by the suggested strategy is provided by the inclusion of these tabulated findings. When combined with the Distributed Pattern-based Neural Network (DPNN) classifier, the suggested DCTP-based texture

extraction significantly improves the model's generalization, accuracy, and resilience, as the table illustrates.

In terms of accuracy, the DCTP-DPNN framework is more effective in the detection of defects in general and more precisely than the current method, where the table and graphical comparisons also testify. This shows the ability of the proposed model to offer a more intelligent and reliable system of tyre inspection that can be used in the real-time industrial setting.

Table 2. Performance evaluation of existing and proposed techniques

Parameter	**YOLOv5 Baseline**	**CNN**	**SVM**	**Proposed DCTP-DPNN**
Sensitivity	0.9326	0.9418	0.9145	0.9862
Specificity	0.9074	0.9205	0.8916	0.9743
Precision	0.9158	0.9312	0.9008	0.9801
F1-Score	0.924	0.934	0.909	0.982
MCC Coefficient	0.897	0.91	0.882	0.975
Recall	0.9326	0.9418	0.9145	0.9862
Accuracy	0.9274	0.9403	0.9061	0.9828
Kappa Coefficient	0.884	0.903	0.876	0.972

To compare the results of the proposed approach with the results of the existing model, which was reported in, the Kappa Coefficient was presented in Figure 5, and the accuracy performance of the suggested model was again confirmed. The use of the Kappa Coefficient is a sure measure of the level of agreement between the real and expected classifications, considering the possibility of chance agreement. It is observed in Figure 8 that the proposed DCTPdpNN model yields a much larger Kappa value, which means that the model provides a high level of agreement between the results projected and the real ground truth labels. The results indicate that the proposed system is much better than the existing system, and the proposed model has a total classification accuracy of nearly 98%. This high level of concurrence is evidence of the strength and reliability of the proposed classifier in accurately detecting flaws in the surfaces of tyres.

In order to measure the effectiveness of the model further, Figure 9 traces the error rate and False Positive Rate (FPR). Error rate indicates the frequency of inaccuracy of prediction by the model. It is calculated as the percentage difference between the accuracy that was obtained and 100%. According to the investigation, the error rate in the proposed system is 2% that is much smaller than the one in the comparison model in [24]. Such a reduction indicates the extent to which the improved texture-based feature extraction and classification scheme provides a reduction of false alarms and misclassifications.

Moreover, the results were validated by the use of the area under the Curve (AUC) statistic, which provides an in-depth evaluation of all the discrimination capability of the classifier under different settings of threshold. The AUC values of Table 3 reveal that the AUC-suggested DCTPDN framework shows a consistently better performance on the other classification models, showing higher power to distinguish between defective and defect-free tyre sections. This high accuracy, stability, and reliability are noted by this enhanced performance, and thus, the improved performance makes the suggested approach suitable for real-time applications of detecting defects in industries.

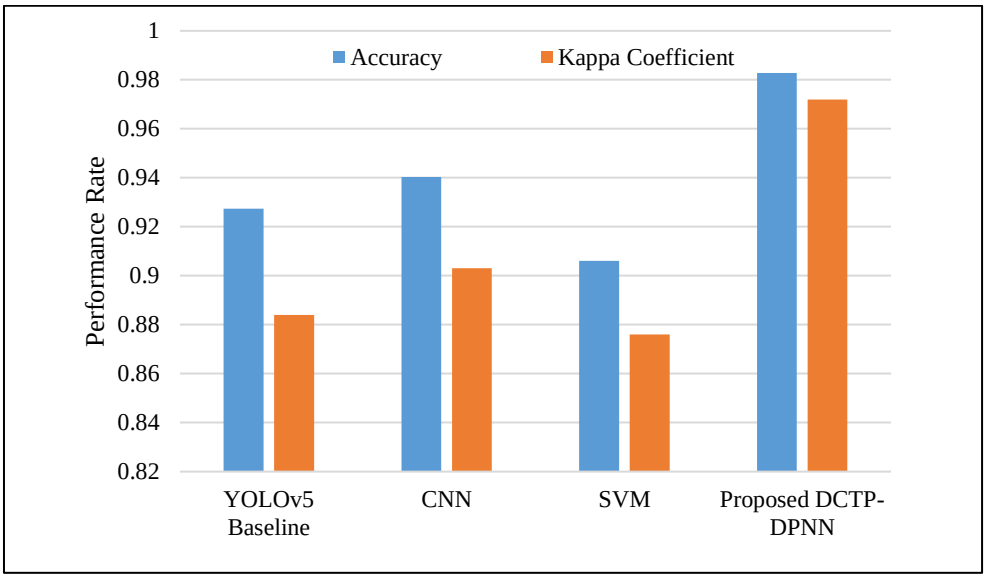

Figure 8. Accuracy and Kappa coefficients

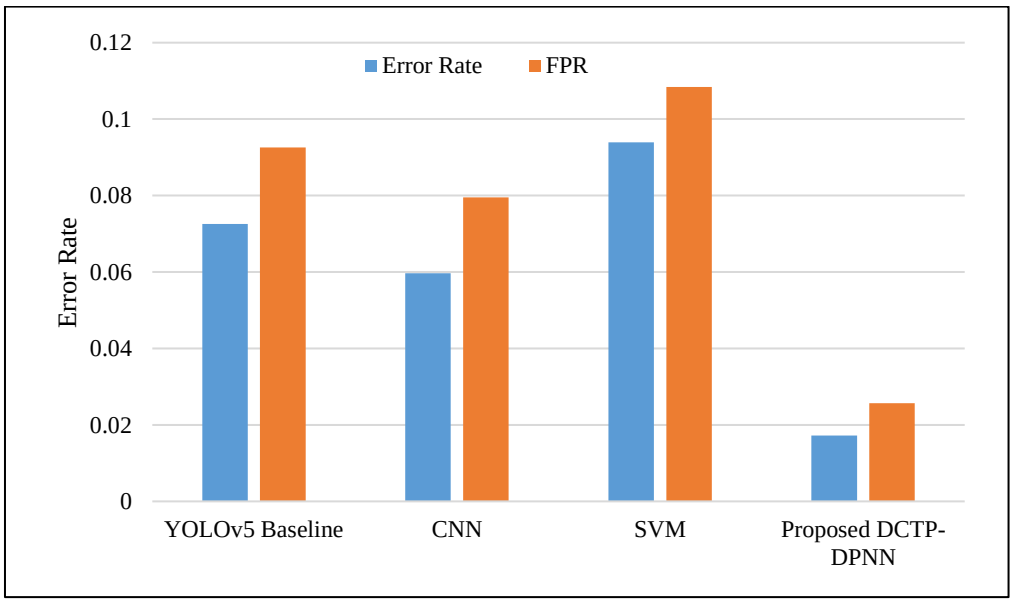

Figure 9. Error rate and FPR

Table 3. AUC analysis

Methods	AUC
YOLOv5 Baseline	0.942
CNN	0.953
SVM	0.936
SoGF-FV	0.961
Proposed DCTP–DPNN	0.985

E. Accuracy Analysis

Table 4 demonstrates a comparison of the accuracy of the classification of various existing feature extraction and prediction models. The comparison proves the gains of the suggested Directional Convoluted Ternary Pattern-Neural Network (DCTP-NN) technique. In comparison with the methods of traditional texture-based classification, the DCTP-NN technique manages to merge deep neural classification and texture pattern extraction, which can offer a more confident representation of local image features even in the face of challenging conditions, such as the instrumentation noise and changes

in illumination. Due to the integrated architecture, the system is able to detect and classify the characteristics with minimal error.

The accuracy is measured by determining the percentages of labels that are detected correctly and are either 0 or 1 (non-defective or defective areas) in the tyre face images, which is an important measure of the classification capability of the model. The larger the accuracy, the higher the knowledge that the system is capable of generalizing across samples of pictures as well as the faults. As depicted in Table 4, compared to recent methods, the proposed DCTP-NN model demonstrates a high classification accuracy increase of approximately 2%. This is in large part due to the adaptive learning abilities of the neural network, as well as directed convolutional processing of the model, which finds fine-grained texture orientations and enhances the decision boundaries between related texture categories.

Altogether, the findings are in favor of the better performance of the proposed DCTP-NN model in dealing with difficult tasks of texture-based classification. To be deployed in real-time industrial vision tasks such as tyre defect and quality inspection, feature extraction based on DCTP and distributed neural classification not only enhances the reliability of prediction but also makes the system more robust, which is demonstrated by the gradual rise in accuracy through different sets of test cases.

Table 4. Accuracy analysis

Methods	**Accuracy**
MDC	91.8
Bayes	92.3
CS	90.7
SoGF-FV	96.1
Proposed	0.98

F. True Positive Rate and False Positive Rate

Figure 9 illustrates the Receiver Operating Characteristic (ROC) curves for the SoGF-FV model and the proposed DCTP–DPNN classification framework, evaluated using the dataset referenced in . The ROC curve shows a graphical depiction of the diagnostic capacity of the classifier by diagrammatically showing the True Positive Rate (TPR) versus the False Positive Rate (FPR) at distinct decision thresholds. In this case, the TPR is the sensitivity of the model that reflects its ability to accurately detect defective samples, and FPR is (1 -Specificity), the rate at which the non-defective samples are falsely classified as defective.

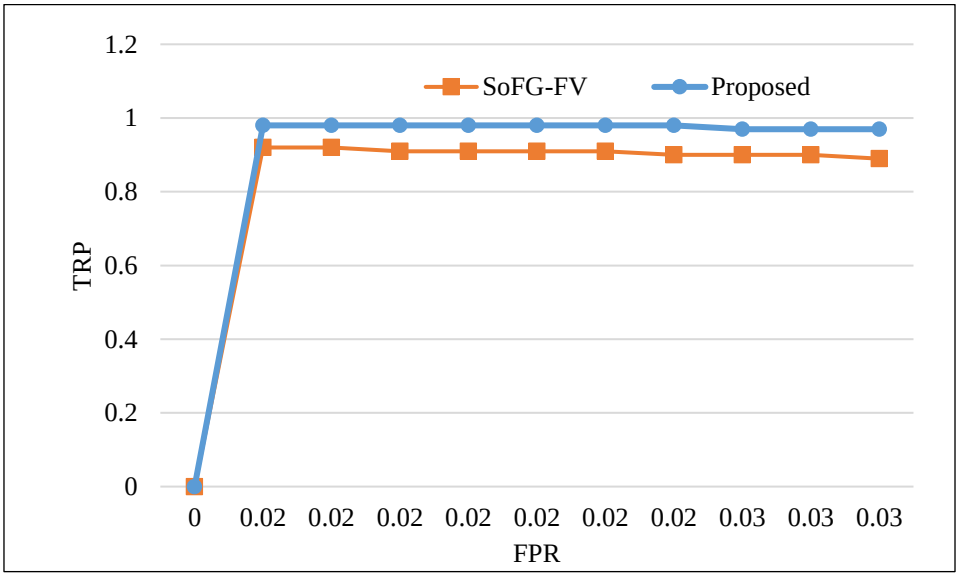

Figure 10. ROC analysis

Observed from Figure 10, the proposed DCTP–DPNN model achieves a higher TPR with a significantly lower FPR compared to the SoGF-FV method, illustrating its superior discriminative performance. The curve of the proposed approach closely approaches the upper-left corner of the ROC space, which denotes maximum sensitivity and minimal false detection. This trend will prove that the offered model has a better balance between sensitivity and specificity and, therefore, reduces the false alarms to a minimum and does not harm the accuracy of detection.

The total area under the ROC curve (AUC) is also useful in upholding the fact that the model has a high potential to differentiate between flawed and non-defective tyre patches. Therefore, ROC analysis proves the effectiveness and reliability of the proposed DCTP-DPNN classification system, and it is a rather effective way of including it in applications related to industrial vision-based fault diagnosis.

An ablation study was done to compare various settings of the proposed DCTP-DPNN model. The differences were made in the use of DCTP based on the use of basic neural networks, DCTP vs. other classifiers such as SVM and CNN, and testing different feature extraction methods such as LBP and HOG. As the results indicated, the combination of DCTP and DPNN was always the most effective and accurate in terms of recall, precision, and F1-score, which points to the strength and efficiency of the given approach.

G. Result Discussion

It is clearly revealed by the general experimental research that the proposed DCTP-based texture feature extraction with the help of the Distributed Pattern-based Neural Network (DPNN) classifier is more successful than both traditional and state-of-the-art methods. The model represents fine-grained local variations in the tyre structure and structural edges and local intensity variations by effectively establishing directional texture patterns with the Directional Convoluted Ternary Pattern (DCTP). Such characteristics are necessary in order to make a clear distinction between defective and non-defective regions. In scenarios where the data set contains noisy or skewed images, the DPNN classifier utilizes such rich features to offer extremely precise label estimates, which is evidence of the strong ability to generate generalization with a relatively small training data set.

Quantitative evaluation uses several statistical measures, including accuracy, precision, recall, F1-Score, Matthews Correlation Coefficient (MCC), Kappa coefficient, sensitivity, specificity, and error rate. All the findings prove that the recommended framework is superior to the existing techniques, such as CNN-based classifiers, SVM, and SoGF-FV models. The ROC study also shows that the proposed method is durable in the accurate detection of tyre issues and minimizes misclassifications, which has the highest sensitivity and a low false positive rate. The DCTP-DPNN approach has its advantages in terms of a reduction in error rate to the lowest possible (2-3 %) and the overall increase in the accuracy of the method (approximately 2-3 %) as compared to the other standard methods.

A combination of these results shows that more advanced texture feature extraction with a distributed neural classification model can provide a more robust, reliable, and efficient way of automated identification of tyre problems. The proposed solution is suitable for real-time industrial implementation and large-scale quality control implementation because it not only enhances the detection of flaws but also ensures the same performance across diverse environmental conditions.

CONCLUSION

The study proposes a state-of-the-art tyre defect detection system that combines the use of Directional Convoluted Ternary Pattern (DCTP) in the extraction of texture features and Distributed Pattern-based Neural Network (DPNN) in the classification. The model proposed has a much better result than the available methods, with an accuracy of 98.28, sensitivity of 98.62, specificity of 97.43, and F1-score of 98.2, showing that the model is able to be useful in the real industry. Besides, the model has a low error rate of 2 % and a high Matthews Correlation Coefficient (0.975), which is another indicator of the strength of the model. The texture extraction technique based on the DCTP enables the model to deal with changes in the illumination, noise, and other types of tyre defects, which pose significant problems

in an industrial setting. The proposed DCTP-DPNN framework has been very successful and has better classification accuracy with fewer training samples, minimizing memory space as well as computation time, as compared to the conventional ones, such as CNN and SVM. This proves that it can be implemented in real time in automated quality control systems. In the future, it is planned to use transformer-based architectures and attention mechanisms that would help to capture long-range spatial correlations and enhance the defect detection ability of the model. Also, the development in extending the flexibility of the system to other industrial processes, like automated checking of images in other manufacturing industries, will be an important direction of development. It might also be possible to investigate the complexification of the model with edge computing to make it process data quicker in situ, increasing the scalability and real-time implementation in resource-constrained settings.

REFERENCES

[1] Kazmi W, Nabney I, Vogiatzis G, Rose P, Codd A. An efficient industrial system for vehicle tyre (tire) detection and text recognition using deep learning. IEEE Transactions on Intelligent Transportation Systems. 2020 Jan 24;22(2):1264-75. https://doi.org/10.1109/TITS.2020.2967316

[2] Mohan P, Pahinkar A, Karajgi A, Kumar LD, Kasera R, Gupta AK, Narayanan SJ. Multi-contrast convolution neural network and fast feature embedding for multi-class tyre defect detection. In2020 4th International Conference on Electronics, Communication and Aerospace Technology (ICECA) 2020 Nov 5 (pp. 1397-1405). IEEE. https://doi.org/10.1109/ICECA49313.2020.9297615

[3] Massaro A, Dipierro G, Cannella E, Galiano AM. Comparative analysis among discrete fourier transform, K-means and artificial neural networks image processing techniques oriented on quality control of assembled tires. Information. 2020 May 8;11(5):257. https://doi.org/10.3390/info11050257

[4] Harshitha A, Samala S. Detection of Tyre Wear Out Using OpenCV and Convolution Neural Networks–Survey. InCommunication Software and Networks: Proceedings of INDIA 2019 2020 Oct 4 (pp. 9-17). Singapore: Springer Singapore.

[5] Zhu J, Han K, Wang S. Automobile tire life prediction based on image processing and machine learning technology. Advances in Mechanical Engineering. 2021 Mar;13(3):16878140211002727. https://doi.org/10.1177/16878140211002727

[6] Raj AA, Kaviarasu S, Saran K, Mohammednatheem F. CNN based Tyre Life Prediction and Defect Identification System. In2021 6th International Conference on Communication and Electronics Systems (ICCES) 2021 Jul 8 (pp. 1-5). IEEE. https://doi.org/10.1109/ICCES51350.2021.9488961

[7] Pahinkar A, Mohan P, Mandal A. Faster region based convolutional neural network and VGG 16 for multi-class tyre defect detection. In2021 12th International Conference on Computing Communication and Networking Technologies (ICCCNT) 2021 Jul 6 (pp. 01-07). IEEE. https://doi.org/10.1109/ICCCNT51525.2021.9579855

[8] Sharan S, Reddy R, Reddy P. Multi-level drowsiness detection using multi-contrast convolutional neural networks and single shot detector. In2021 international conference on intelligent technologies (CONIT) 2021 Jun 25 (pp. 1-6). IEEE. https://doi.org/10.1109/CONIT51480.2021.9498568

[9] Rajeswari M, Julie EG, Robinson YH, Joseph E, Arun AS, Sebastian E, Kumar R, Long HV, Son LH. Detection of tyre defects using weighted quality-based convolutional neural network. Soft Computing. 2022 May;26(9):4261-73.

[10] Zhang Q, Zhang P, Lv C, Jiang Q, Dong R, Zhang X. Aminomethylated Lignin as a Multifunctional Bio-based Reinforcer for Natural Rubber with Enhanced Mechanical Strength, Steel–Cord Adhesion, and Anti-Aging Performance. Steel–Cord Adhesion, and Anti-Aging Performance.

[11] Ding Z, Zhou J, Du G, Zhao S, Furukawa T, Lu K. A two-model automatic towel defect detection method based on YOLOv5. 2022:386–393.

[12] Yang S, Jiao D, Wang T, He Y. Tire speckle interference bubble defect detection based on improved faster RCNN-FPN. Sensors. 2022 May 21;22(10):3907. https://doi.org/10.3390/s22103907

[13] Wang Y, Wang W. Generative adversarial network-based data augmentation for tyre surface defect detection. In2023 IEEE 19th international conference on automation science and engineering (CASE) 2023 Aug 26 (pp. 1-6). IEEE. https://doi.org/10.1109/CASE56687.2023.10260675

[14] Peng C, Li X, Wang Y. TD-YOLOA: An efficient YOLO network with attention mechanism for tire defect detection. IEEE Transactions on Instrumentation and Measurement. 2023 Sep 7; 72:1-1. https://doi.org/10.1109/TIM.2023.3312753

[15] Taspinar YS. Predicting Defective and Good Tyre Quality Status with Pre-Trained CNN Models. In2023 International Conference on Modeling, Simulation & Intelligent Computing (MoSICom) 2023 Dec 7 (pp. 510-514). IEEE. https://doi.org/10.1109/MoSICom59118.2023.10458796

[16] Liu H, Jia X, Su C, Yang H, Li C. Tire appearance defect detection method via combining HOG and LBP features. Frontiers in Physics. 2023 Jan 12; 10:1099261. https://doi.org/10.3389/fphy.2022.1099261

[17] Kaushik P, Kukreja V, Chabbra R, Saini R. Smart Tyre Monitoring: Unleashing the Power of InceptionV3 for Accurate Defect Detection. In2024 International Conference on Big Data Analytics in Bioinformatics (DABCon) 2024 Nov 21 (pp. 1-6). IEEE. https://doi.org/10.1109/DABCon63472.2024.10919380

[18] Kaushik P, Kukreja V, Chabbra R, Saini R. Deep Learning-Based Tyre Quality Classification Using ResNet50: A Robust Approach for Automated Inspection and Defect Detection. In2024 International Conference on Augmented Reality, Intelligent Systems, and Industrial Automation (ARIIA) 2024 Dec 20 (pp. 1-5). IEEE. https://doi.org/10.1109/ARIIA63345.2024.11051778

[19] Orowho FO, Vincent RO. A comparative study of CNN-based feature extraction and machine learning classifiers for identification of tyre defect. In2024 IEEE SmartBlock4Africa 2024 Sep 30 (pp. 1-7). IEEE. https://doi.org/10.1109/SmartBlock4Africa61928.2024.10779556

[20] Singh P, Hasija T, Ramkumar K. Enhancing Tyre Quality Assessment with Cutting-Edge Classification Algorithms. In2024 8th International Conference on Electronics, Communication and Aerospace Technology (ICECA) 2024 Nov 6 (pp. 1253-1259). IEEE. https://doi.org/10.1109/ICECA63461.2024.10801014

[21] Saleh RA, Ertunç HM. Attention-based deep learning for tire defect detection: Fusing local and global features in an industrial case study. Expert Systems with Applications. 2025 Apr 15;269:126473. https://doi.org/10.1016/j.eswa.2025.126473

[22] Yuan H, Yuan M, Wang Q, Qiao J, Su Z. Tire-YOLOv11n: a lightweight and efficient deep learning model for real-time tire defect detection in natural lighting environments [preprint]. 2025 Aug 29. Available from: SSRN 5415444.

[23] Saleh RA, Ertunç HM. Attention-based deep learning for tire defect detection: Fusing local and global features in an industrial case study. Expert Systems with Applications. 2025 Apr 15;269:126473. https://doi.org/10.1016/j.eswa.2025.126473

[24] Li X, Peng C, Li X, Zeng G, Chu F. Fault Detection for Impurities and Cord Defects Based on Radial Tire X-ray Images. In2025 37th Chinese Control and Decision Conference (CCDC) 2025 May 16 (pp. 5172-5177). IEEE.